Int. J. Electrochem. Sci., 9 **(2014)** 1087 - 1101

International Journal of
ELECTROCHEMICAL
SCIENCE
www.electrochemsci.org

The Impact of Metal Inert Gas Welding on the Corrosion and Mechanical behavior of AA 6061 T6

E. Mahdi[*], *E. O. Eltai, A. Rauf*

Qatar University. Department of Mechanical and Industrial Engineering, P.O. Box 2713, Doha, Qatar.
[*]E-mail: Elsadigms@qu.edu.qa

Received: 8 September 2013 / *Accepted:* 13 November 2013 / *Published:* 5 January 2014

An attempt has been made to investigate the effects of MIG welding on the corrosion and mechanical properties of AA 6061 T6. A series of experimental techniques has been conducted to evaluate the corrosion and mechanical properties of the alloy. The corrosion media used was 3.5% (wt) NaCl. Polarization and open circuit potential tests were conducted by exposing various zones independently; therefore the reported corrosion results correspond to uncoupled condition. Different mechanical tests including tensile, torsion, and hardness were carried out; the same tests were also used for the un-welded specimens. The results show that the heat affected zone (HAZ) exhibited poor corrosion properties compared to the base metal (BM). The corrosion on both HAZ and BM was of pitting nature. More corrosion was observed on HAZ due to the thermal effects of the welding. Corrosion potential of HAZ was largely fluctuated comparing to BM with more negative peaks. The corrosion potential of the BM remained relatively steady over the whole immersion time. Welded specimens show lower mechanical properties comparing to non-welded specimens. The location of failure for welded and un-welded specimens after tensile test was found to be across the centre of the specimens. Welded tensile specimens have shown lower tensile strength. The location of the failure for welded specimens after torsion test was found predominantly along the HAZ which was attributed to the microstructural alteration that caused by the generation of heat during the welding process. Un-welded torsion specimens were failed near the centre line. Welded specimens exhibited lower torsion properties compared to the non-welded specimens with a reduction of almost 50%. The lowest hardness value was found across the weld centre.

Keywords: MIG, HAZ, Mechanical properties, Pitting corrosion, BM

1. INTRODUCTION

Due to the diverse applications of Aluminium and its alloys in automobile and aerospace industries[1] many researchers are now focusing on finding the best type of welding to join these

important materials. The behavior of welded AA in different environment is of paramount importance. However, more research is needed to fully understand the properties of these materials and its behavior. Research is also needed to overcome their limitations.

Welding is the main joining method for these materials. Many welding methods for Aluminium and its alloys have been reported [2,3,4], these methods include tungsten arc welding (TIG), metal inert gas welding (MIG), laser welding, and friction stir welding (FSW). It is widely accepted that the mechanical and corrosion properties of welded Aluminium alloys are influenced by the welding process. Welding process exhibited a partially melted zone (PMZ), in other words heat affected zone (HAZ) adjacent to the fusion zone (FZ) where the metals melt and solidify, beyond the HAZ is that part of the metal which has not been subjected to thermal alteration and it is called the base or parent metal (BM). The formation of these zones is usually caused by the heat generated during the welding process. Such heat may alter the microstructure of AA [5]. Wadeson et al [6] found that the corrosion resistance of the welded materials at different regions that formed during the welding process is not the same; their study showed that the welded zones of most joints are susceptible to corrosion. Welding of Aluminium and its alloys is considered to be challenging because lots of difficulties are associated with this kind of joining, the main important difficulties are related to the presence of oxide film on the surface, high thermal conductivity, solidification shrinkage, formation of defects, and more important is the solubility of hydrogen and other gases in molten state [7]. The presence of these difficulties and challenges has motivated us to conduct the current research and others in order to have a better understanding.

MIG welding has been used widely to join pieces of aluminium alloys in construction of rail vehicles, ships, steel bridges, and pressure vessels [8]. In the MIG welding process [9], a gas shield is usually used to protect the arc and the weld from atmospheric contamination, an electric potential is established between the electrode and the work piece that needs to be welded, such electric potential will cause the current to flow and consequently a thermal energy will be generated in the partially ionised inert gas.

In the first paper in this series [10] the influence of TIG welding on the corrosion and mechanical properties of AA 6061 T6 was investigated, it was found that TIG welding causes the alloy to be more susceptible to corrosion particularly the HAZ which is in agreement with the work that done by many authors [6,11-13], the welding was also found to reduce the mechanical properties of the alloy which was attributed to the modification and softening induced in the alloy . Therefore, it is considered important to carry on investigating the effects of different types of welding on the same alloy, plans were set to compare between different types of welding in order to expand the scientific knowledge in this important research area.

This paper is focusing on the effects that MIG welding may have on the corrosion and mechanical properties of AA 6061 T6, the corrosion behavior was tested in 3.5% (wt) NaCl solution. Different electrochemical and mechanical techniques were used.

2. EXPERIMENTAL PROGRAM

2.1 Welding process

The material used in this study was AA 6061 T6, the composition of the alloy is presented in table 1.The metal inert gas arc welding (MIG) method was used to weld the specimens. Commercial welding machine with a capability of changing its electric current was used. Circular specimens were welded under Ar (99% purity) as a shielding gas. A current of 110 Ampere using Telwin Master MIG machine was applied.

Table 1. Chemical composition of Al alloy 6061 T6

Metal	Al	Si	Mg	Cu	Cr	Mn	Zn	Ti	Fe
(Wt%)	95.8-98.6	0.4-0.8	0.8-1.2	0.15-0.4	0.04-0.35	Max 0.15	Max 0.25	Max 0.15	Max 0.7

The type of filler used was a commercial A404 Aluminium wire. The chemical composition of the wire is presented in table 2. To remove any contaminants (oil, grease etc..) that may present as a result of the cutting or handling process, the work pieces were wiped with ethanol before being welded.

Table 2. Chemical composition of commercial A404 wire

Metal	Si	Mg	Cr	Fe	Ti	Cu	Mn	Al
Wt %	0.1	4.72	0.06	0.34	0.06	0.01	0.06	Balance

2.2 Corrosion test

To compare the corrosion behavior of the HAZ and the BM, corrosion potential and Potentiodynamic polarization were evaluated independently by separating these zones from the weld joint, tests were carried out using Gamry potentiostat DC105. The scan rate was 1.00 mV/s. Samples were then put in a cell containing the NaCl solution. Corrosion potential was monitored over a period of 4 hours. A three electrode cell was used, the three electrodes being the separated HAZ and BM as working electrode, saturated calomel as reference electrode, and a graphite counter electrode. Experiments were conducted at room temperature which is approximately (20±1°C).

2.3 Mechanical tests

2.3.1 Tensile test

Specimens for tensile testing were machined to ASTM E8-04 standards. A CNC milling machine was used to cut the specimens into the specified dimension. Tensile test was conducted using

a computer controlled testing machine (Instron, Model 5585H) with a capacity of 250 KN and a cross head speed of 5 mm/min. Figure 1 is showing the configuration of the specimens used for tensile test.

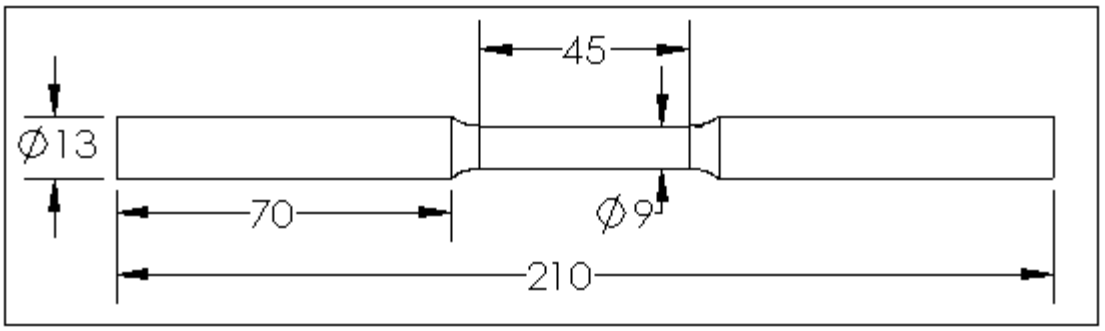

Figure 1. Dimension of specimen used for tensile test (mm)

2.3.2 Hardness test

Rockwell hardness test was made as per ASTM E18-05 standard. Hardness test was carried out on circular welded samples with a load of 60 kg, a ball indenter of 1/16 inch diameter, and duration of 15s using Indentec hardness tester Model 8187.LKV. Four different readings were taken around the welded circular area; the same number of readings was then taken at an interval of 5mm away from the welded area.

2.3.3 Torsion test

Specimens for torsion test were prepared as per ASTM E143-87 standard. Test was carried on welded and un-welded specimens using a computer controlled machine (Jinan testing machine, model NDW-2000) with a rotation speed of 90°/min. Figure 2 is showing the configuration of the torsion specimen used.

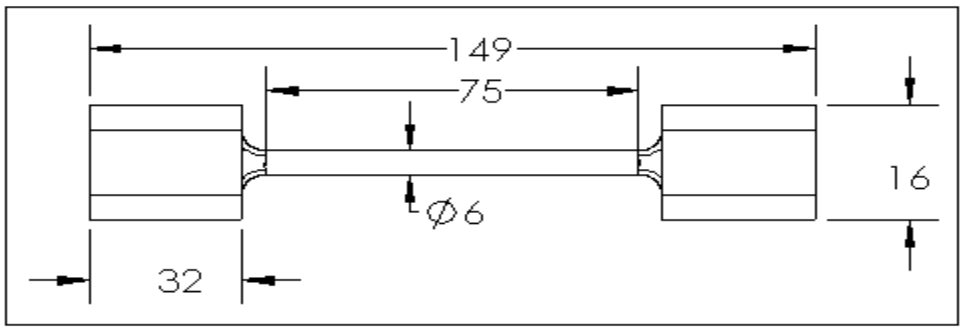

Figure 2. Dimension of specimen used for torsion test (mm)

3. RESULTS AND DISCUSSION

3.1 Corrosion behavior

Aluminium and its alloys are well known of their sensitivity to chlorides environment suffering pitting corrosion [14], the extent of pitting corrosion is depends on many factors including but not limited to the solution type, its corrosivity, temperature at which the test is conducted, and the immersion time. In this research article a series of corrosion and mechanical tests were conducted in order to investigate the effects of commercial MIG welding on the properties of Aluminium alloy 6061 T6. Tests were conducted carefully at room temperature and repeated many times in order to have a reproducible data. The corrosion behavior was evaluated by immersing the specimens in 3.5% NaCl solution and via morphological analysis of the surface using optical microscope and Scanning Electron Microscopy (SEM). Figure 3 is an example of a potentiodynamic polarization plot for the BM and the HAZ. It can be seen that the base metal has a corrosion potential of -0.725V and a corrosion current of 24.02 μA. It can also be seen that the corrosion potential of the heat affected zone was -1.238 V and the corrosion current was 94.86 μA. From figure 3 it is apparent that the corrosion resistance of the heat affected zone is less than the base metal. The effects of microstructure on corrosion rate is significant, studies show that heterogeneous microstructure can reduce the corrosion properties, this fact is reflected in the corrosion behavior of the HAZ as shown by the Potentiodynamic plots in figure 3, it is obvious that the heat that generated during the welding process causes the HAZ to have poor corrosion properties. As expected the nature of corrosion for both the HAZ and the BM was pitting corrosion for all specimens.

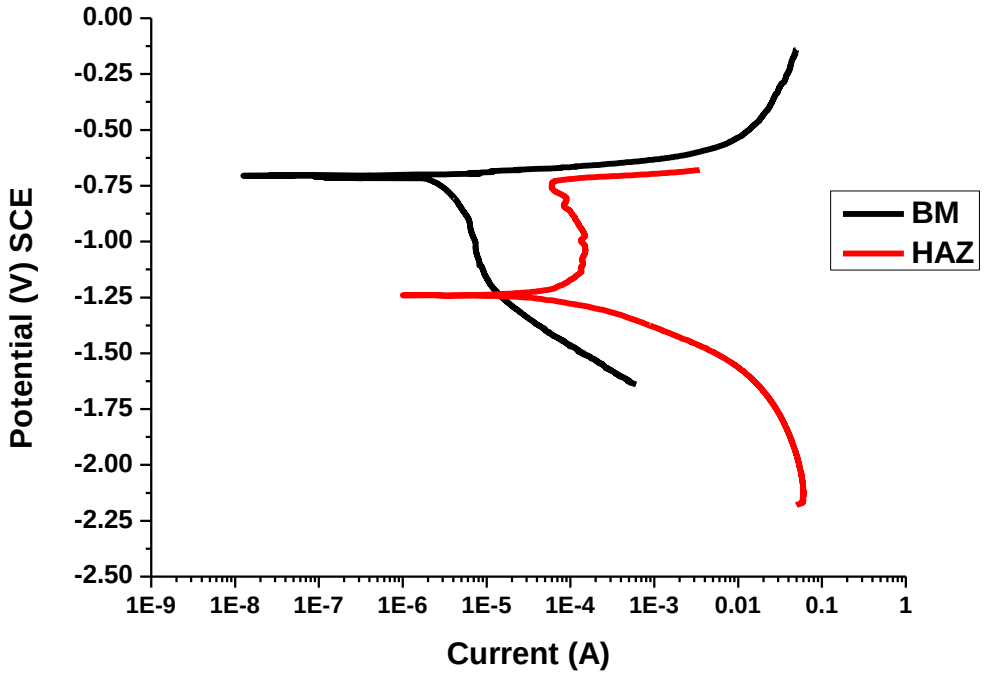

Figure 3. Potentiodynamic plots for heat affected zone (HAZ), and base metal (BM) of AA 6061 T6 in 3.5 (wt%) NACl solution

It is widely accepted that the value of the corrosion potential of a metal in an aqueous solution offers very little information about the mechanism of the reaction and the rate controlling factor. However, combining corrosion potential data with other facts can often provide useful information about the corrosion process [15].The open circuit potential curves for BM and HAZ are shown in figure 4, it is obvious that the HAZ exhibited more cathodic values compared to the BM in the first 2000 seconds indicating poor corrosion behavior. It was noted that the corrosion potential for HAZ was initially around -1.06 V, decreasing to around -1.12 V, which afterwards increased to around -0.84 V after 1100 seconds of immersion. Moreover, potential of the HAZ was largely fluctuated over the whole immersion time compared to a relatively stable potential values for the BM. Furthermore, the potential curve which was observed for longer period (14400 seconds) showed that even with longer exposure time the BM exhibited relatively steady potential values. The potential of the HAZ started to shift in the negative direction between 8000 and 10000 seconds. The anodic behavior that shown by the HAZ was attributed to the attack of the Aluminium oxide film by the corrosive media (3.5 wt% NaCl) and also to the modified microstructure of the HAZ as a result of the welding process [12,14,16,17].

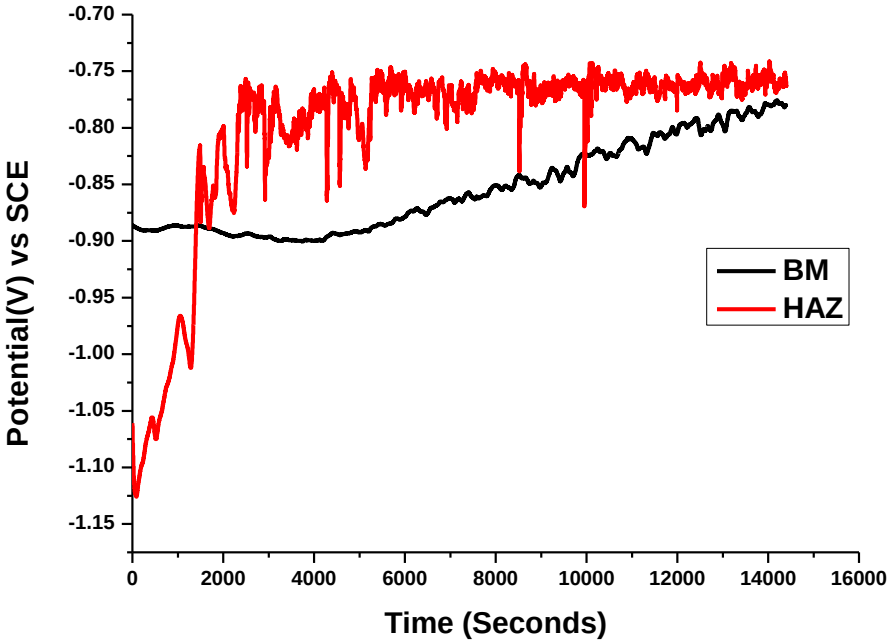

Figure 4. Corrosion potential for heat affected zone (HAZ), and base metal (BM) of AA 6061 T6 in 3.5 (wt%) NACl solution

The open circuit potential results which were shown by figure 4 correlated well with the extent of corrosion on the HAZ and BM, it was noted that the number and the size of pits were much bigger on the HAZ whereas relatively small and less pits were observed on the BM (figures 5 and 6). This observation is consistent with many studies [18,19].

On the basis of the above mentioned facts, it can be said that the potential of the HAZ was largely fluctuated after exposure to aggressive 3.5% NaCl solution which is an indication of poor corrosion resistance whereas the BM specimens have shown relatively better corrosion resistance.

Generally, it can be said that movement of the corrosion potential in the noble direction which was the case in the BM is an indicative of an increasing cathodic/anodic surface area ratio, and it can also be considered as a sign that oxygen and other corrosive species were penetrated the Aluminium oxide film and reached the metal surface. On the other hand, movement of corrosion potential in the active direction which is the case in the HAZ is an indication of increasing anodic/cathodic surface ratio and thus the overall corrosion rate is becoming significant [20].

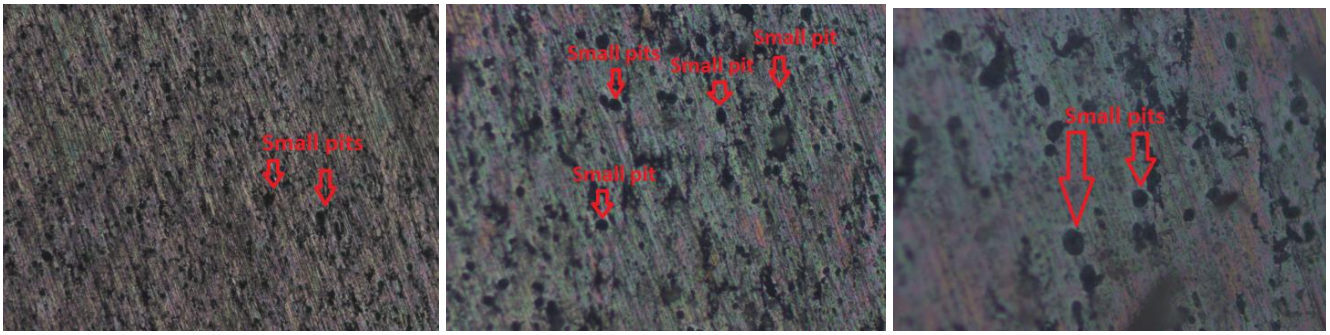

(A) (B) (C)

Figure 5. Extent of corrosion on the BM after immersion in 3.5% NaCl solution at different magnification (A) 10X, (B) 20X, and (C) 50X

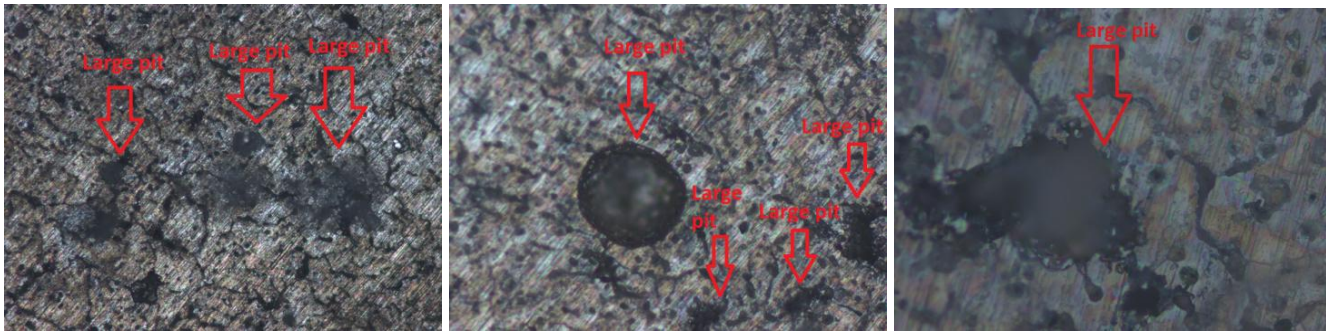

(A) (B) (C)

Figure 6. Extent of corrosion on HAZ after immersion in 3.5% NaCl solution at different magnification (A) 10X, (B) 20X, and (C) 50X

3.2 Tensile behavior

The tensile strength of MIG welded and Un-welded specimens were evaluated. The results obtained in the current study clearly reveal that the tensile strength of AA 6061 T6 has been decreased considerably due to the welding process. This was shown to be caused by the heat input during the welding process which caused fusion of the welded zone and the partially melted zone (PMZ), considerably microstructural changes have taken place. The data extracted from stress strain curve are shown in table 3. Based on the ultimate tensile strength (UTS) values for the welded and non welded specimens, it can be said that the welded specimens have shown lower tensile strength compared to the non welded specimens. The non-welded specimens offered comparatively higher yield strength, fracture strength, elongation (%), and reduction in area (%).

Table 3. Tensile properties for MIG welded and un-welded specimens

Tensile property	Ultimate tensile strength (MPa)	Yield stress (MPa)	Fracture stress (MPa)	Elongation (%)	Reduction in area (%)
MIG welded specimen	155.725	127.525	143.43	5.56	10.0043
Un-welded specimen	357.747	322.75	321.373	12.1	32.9

Figure 7 is showing the tensile stress vs strain for welded and un-welded specimens; it is obvious that due to the welding process the tensile strength for welded specimens was significantly reduced to less than 50% compared to non welded specimens. It was expected that the welded specimens will be weaker than the un-welded ones because the welding process may resulted in the presence of voids and defects at the welded zone [9] which was the case in this study.

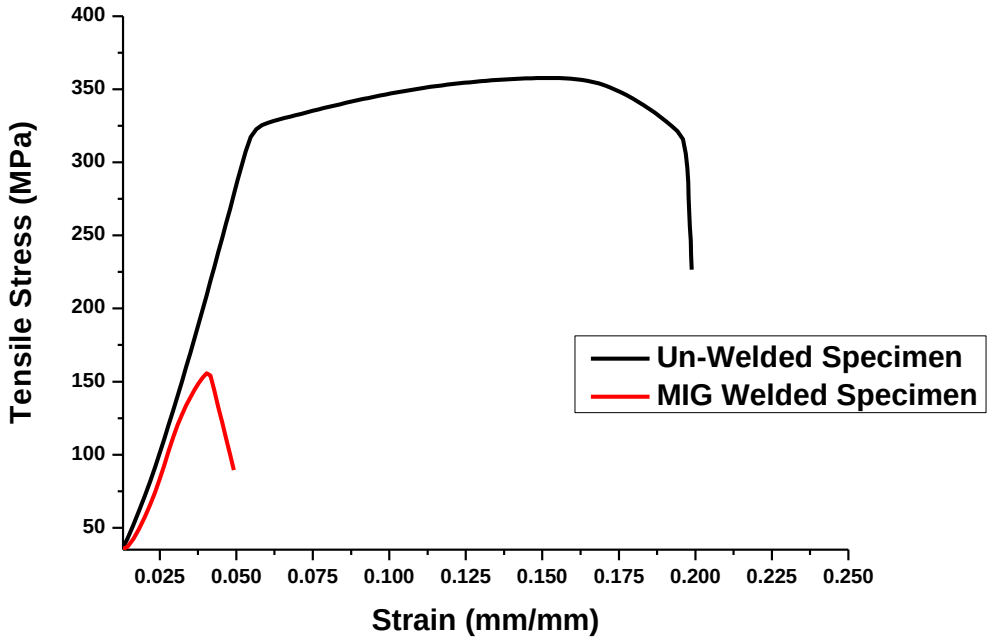

Figure 7. shows stress vs strain plot for welded and un-welded specimens

After the tensile test, the failed specimens were examined with SEM. It was found that the welded zone contains many defects and voids, consequently it shows lower tensile properties compared to the non-welded ones as shown in figure 8.

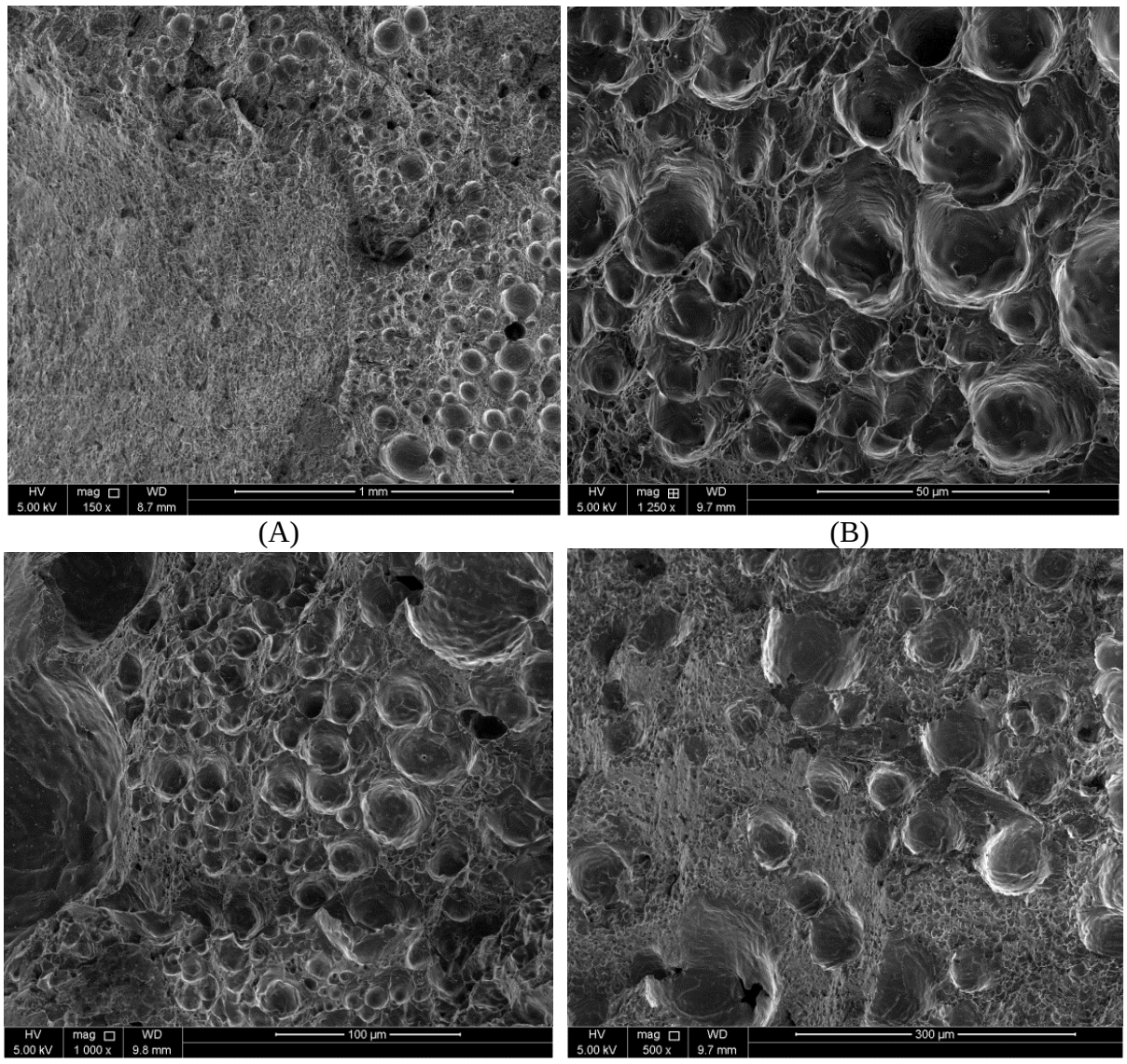

Figure 8. SEM images of welded zones with different magnification after tensile test

Due to the microstructural changes, the tensile strength and the elongation percentage were decreased. The microstructural alterations were also reflected in the electrochemical behavior of the HAZ as demonstrated in figures 3, 4, 5, and 6. It is obvious from the magnitude of the corroded areas (black spots) that the corrosion resistance of the HAZ was much less than the BM.

The microstructure corresponding to the welded zone is presented in figure 8, a,b,c, and d. The detailed microstructure observed at various regions is shown as well. Large and deep voids with big distance between them were present on the welded zone. Consequently, the tensile properties of welded specimens were very low. Another observation was that all welded specimens were broken at the welded zone suggesting that this area has low mechanical properties capability than the rest of the tensile specimen. At the broken location the welded area was coarse, this can be interpreted as that the weldment did not penetrate the base metal well and this could be the reason for the brittle like failure in this region [21].

3.3 Hardness test

Hardness test is a vital test when it comes to the evaluation of mechanical properties of a metal or an alloy. In this research study hardness test was performed to assess the effects of the welding process on different areas. The variations in the hardness that measured across the welded specimen are shown in table 4 and figure 9. The hardness profile from the weld centre towards the base metal shows an increase. The highest value of 117.6 HRF was recorded at a distance of 25mm away from the weld centre. Surprisingly, the lowest value was found to be at the weld centre (25.13 HRF). After that hardness values were increased steadily as we moved away from the welded zone (figure 9), the probable explanation for that is the large voids and defects that observed on the welded zone (figure 8), such defects may lowered the hardness and caused the welded zone to be relatively soft. These results indicated that the welded region is the weakest zone which is in accordance with the study that conducted by Venugopal et al [19]

Table 4. Hardness values for welded specimen

Distance (mm) away from the weld centre	0	5	10	15	20	25
Hardness value (HRF)	25.13	36.3	42.1	72.8	98.13	117.6

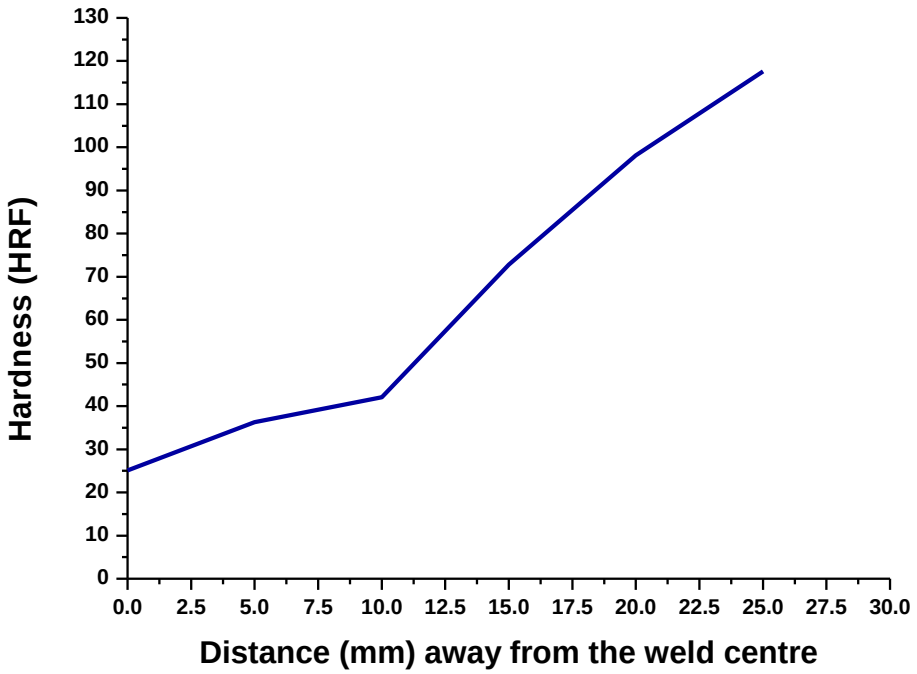

Figure 9. Hardness profile for welded area and away from the weld

3.4 Torsion behavior

Figure 10 shows that the welding process has tremendous effects on the torsion properties of AA 6061 T6 specimens. It is clear that the torque for welded specimens was approximately 6 Nm compared to 12 Nm for the non-welded specimen. It is widely accepted that during the welding process the temperature of the weld centre is higher than the melting point of the alloy [14] and the microstructure of the weld joint changes greatly. It was noted that the welded specimens were broken at the HAZ suggesting that the thermal effects of the welding caused this area to be soft and more susceptible to breakage. This effect is considered one of the drawbacks of conventional welding methods despite getting reasonable mechanical properties comparing to other welding methods. In this series of publication we are trying to reduce the negative effects of the high heat that generated during the welding process by using other welding techniques such as stir friction welding. Furthermore, previous works that conducted by E. Eltai et al [10] showed that the HAZ which developed as a result of the generated heat during the welding process is more susceptible to corrosion.

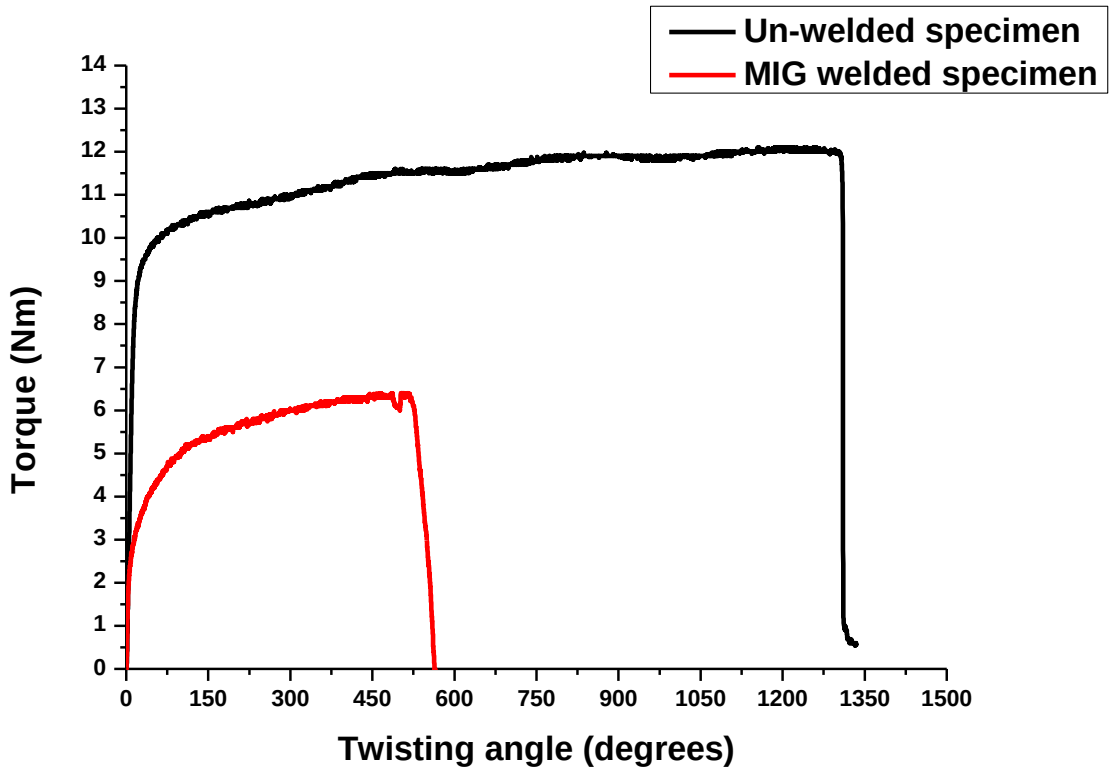

Figure 10. Typical torque vs twisting angle for welded and un-welded specimens

3.5 Failure morphology

It was noted that both welded and un-welded tensile specimens were broken in the middle. The rupture mode for welded specimens revealed two types fracture topography 45° and 90° type (Figure 11 A and B respectively). The visual inspection of the failed un-welded specimens after tensile test revealed V type rupture mode (figure 11 C). The SEM fractographs of the failed welded specimens

clearly reveals the presence of large pores and columnar dendrites within the pores (figure 12 A).The pores was distributed randomly all over the fractured surface indicating poor mechanical properties [7, 14, 22-24]. SEM fractograph of un-welded tensile specimen (figure 12B) clearly shows high resistance to tensile, this is supported by the tensile strength data that shown in table 3.

(A) (B) (C)

Figure 11. Failed tensile specimens (A) MIG welded, (B) MIG welded, and (C) un-welded

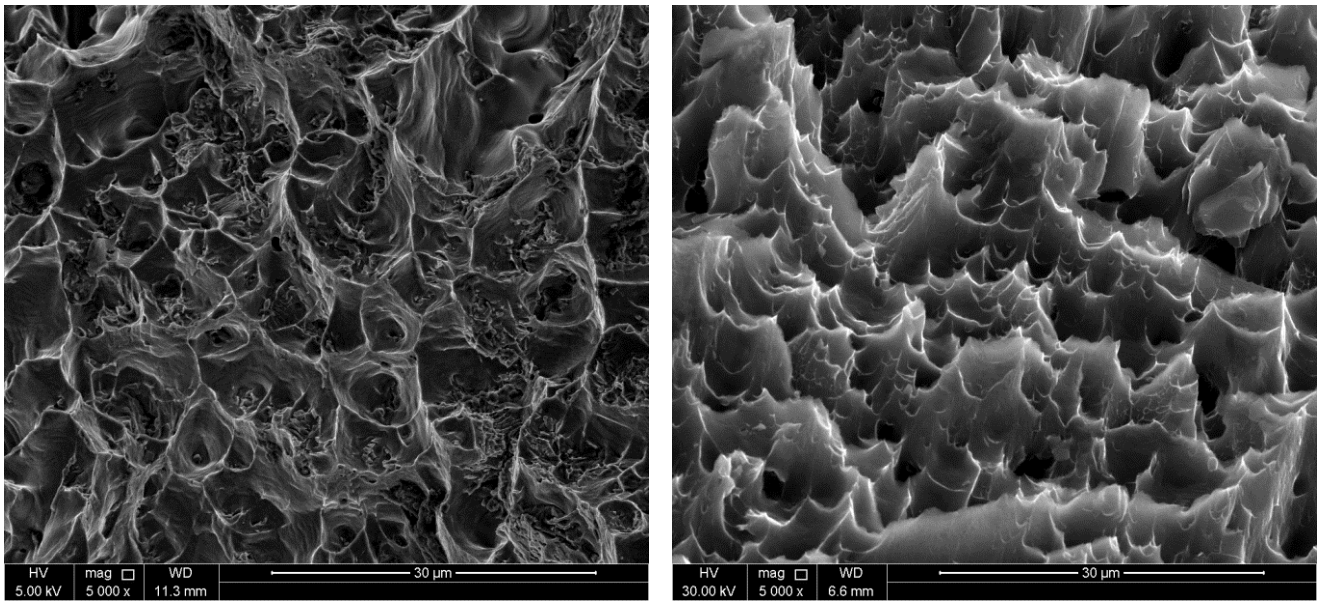

(A) (B)

Figure 12. Fracture morphology of (A) MIG welded and (B) un-welded specimens after tensile test

For torsion test, the location of the failure for welded specimens was found predominantly along the HAZ which was attributed to the microstructural changes that caused by the generation of heat during the welding process (figure 13 A). It was noted that the twisting angle for welded specimens was around 580° whereas the twisting angle for un-welded specimens was approximately 1331° indicating high resistance to torsion comparing to the welded ones, this is supported by the image of the non-welded specimens (figure 13 B) which demonstrated that the failed specimens were twisted due to high resistance to torsion.

(A) (B)

Figure 13. Failed torsion specimens: (A) MIG welded, and (B) Un-welded

The fracture morphology of welded and un-welded specimens after torsion test is presented in figures 14 A,B. coarse dimples surrounded by minor size dimples are the dominant feature of the fractured welded specimens, these dimples are due to the fusion nature of the MIG welding technique [9]. Fine grains located close to each other are obvious which is very similar to the base metal. However, the fractured surface was generally inhomogeneous. It should be pointed out that the nature of the fractured surface of the un-welded specimens as in figure 14 B was more homogeneous.

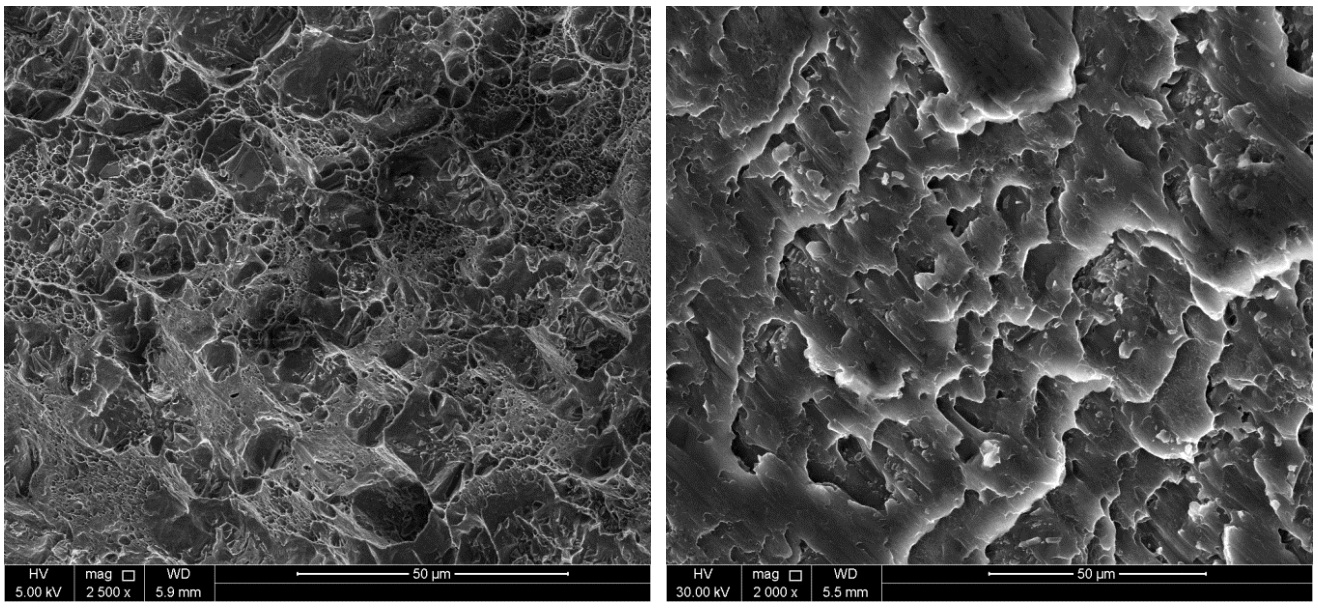

(A) (B)

Figure 14. Fracture morphology of (A) MIG welded, and (B) un-welded specimens after torsion test

5. CONCLUSION

The behavior of MIG welded and un-welded AA 6061 T6 were investigated using a series of electrochemical measurements and mechanical tests. Based on the results obtained in the current research study the following conclusions have be withdrawn:

- The corrosion potential of the HAZ was largely fluctuated over the immersion time showing more negative potential peaks
- Pitting corrosion is dominant on both BM and HAZ
- The HAZ was more susceptible to corrosion showing severe pitting corrosion comparing to the BM
- The tensile strength of welded specimens was reduced to less than 50% due to the effect of welding
- Welded specimens were shown to have lower torsion properties comparing to the non-welded ones with a reduction of almost 50%
- The hardness of the welded specimens was increased as we moved away from the weld centre
- Tensile welded and un-welded specimens were broken at the same place (centre point)
- SEM results reveals large pores and defects on fractured tensile specimens
- Torsion welded specimens were broken at the HAZ suggesting softness of this area due to the impact of MIG welding

ACKNOWLEDGEMENT
This paper was made possible by NPRP grant No. 09-211-2-089 from Qatar National Research Fund (a member of Qatar foundation). The statements made herein are solely the responsibility of the authors.

References

1. M. Jariyaboon, A.J. Davenport, R. Ambat, B.J. Connoly, S.W. Williams, D.A. Price. *Corr Sci*. 49 (2007) 877
2. H.B. Cary, Modern welding technology. Prentice-Hall, Upper Saddle River, NJ (1989)
3. G. Mathers, The welding of Aluminium and its alloys. Woodhead publishing Ltd and CRC Press LLC (2002)
4. A. Kumar, S. Sundarrajan. *Int. J. Adv. Manuf. Technol*. 42 (2009) 118
5. M.P. Groover. Fundamental of modern manufacturing, materials, processes and systems. 3rd Edition. John Wiley and Sons; (2007)
6. D. A. Wadeson, X. Zhou, G.E. Thompson, P. Skeldon, L.D. Oosterkamp, G. Scamans. *Corr Sci*. 48 (2006) 887
7. R.P. Matrukanitz. Selection and weldability of heat treatable aluminium alloys, ASM Handbook-Welding, Brazing and Soldering 6 (1990)
8. W. Xu, M.F. Gittos. Material and structural behavior of MIG butt weld in 6005-T6 aluminium alloy extrusion under quasi-static and impact loading. TWI report No. 14054/1/04; (2004)
9. P.M.G.P Moreira, M.A.V. de Figueiredo, P.M.S.T. de Castro. *Theor. App. Frac. Mech*. 48 (2007) 169
10. E. Eltai, E. Mahdi, A. Alfantazi. *Inter. J. of Electro. Sci*. 8 (2013) 704
11. A.C. Munoz, G. Ruckert, B. Huneau, X. Sauvage, S. Marya. *J. Mat. Proc. Tech*. 197 (2008) 337.

12. V. Fahimpour, S.K. Sadrnezhaad, F. Karimzadeh. *Mater and Des*. 39 (2012) 329.
13. T.S. Kumar, V. Balasubramanian, M.Y. Sanavullah. *Mater and Des*. 28 (2007) 2080.
14. S. Maggiolino, C. Schmid. *J. Mat. Proc. Tech.*. 197 (2008) 237.
15. H. Leidheiser. Prog. Org. Coat. 7 (1979) 79.
16. Y. Dongxia, L. Xiaoyan, H. Dingyong, H. Hui, Z. Liang. *Mater and Des*. 40 (2012) 117.
17. Y. Zha, T. Moan. Thin-Walled Structures. 39 (2001) 631.
18. Z. Nikseresht, F. Kaimzaden, M.A. Golozar. *Mater and Des*. 31 (2010) 2643.
19. A.Venugopal, K. Sreekumar, V.S. Raja. *Metallurgical. Mat. Trans*. 43 (2012) 3135 .
20. E.O. Eltai, J.D. Scantlebury, E.V. Korleva. *Prog. Org. Coat*. 73 (2012) 8.
21. A. Ahmed, M.A. Bakar. *Mat and Desi*. 32 (2011) 5120.
22. M.N. James, G.R. Bradley, H. Lombard , D.G. Hattingh. *Fati. Frac. Eng. Mat.Struc*. 28 (2005) 245.
23. D. Fersini, A. Pirondi. *Eng. Frac. Mecha.*. 75 (2008) 790.
24. G. Bussu, P.E. Irving. *Inter. J. Fati*. 25 (2003) 77.